A New Region Growing-Based Method for Road Network Extraction and Its Application on Different Resolution SAR Images

Pingping Lu, Kangning Du, Weidong Yu, *Member, IEEE*, Robert Wang, *Senior Member, IEEE,* Yunkai Deng, *Member, IEEE*, and Timo Balz, *Member, IEEE*

***Abstract*—Road network extraction plays an irreplaceable role in the applications of synthetic aperture radar (SAR) images. In this paper, we propose a new method based on the region growing to quickly extract the road network, which is suitable for different resolution SAR images. First, a weighted ratio line detector (W-RLD) is proposed to extract road features. Then, an automatic road seeds extraction method, which merges the ratio and direction information, is utilized to improve the quality of the extracted road seeds. Finally, the region growing concept is adopted to construct the road network, and a fast parameter selection procedure is presented for adaptively adjusting growing parameters. In experiments, four kinds of SAR images are used to assess the performance of the proposed method, including Envisat ASAR (30 m), HJ-1-C (5 m), TerraSAR-X (3 m), and airborne C-band data (0.5 m). Both visual and quantitative evaluation results show the adaptability and efficiency of the proposed approach.**

***Index Terms*—Region growing, road extraction, road seed extraction, synthetic aperture radar (SAR).**

I. Introduction

AS AN ESSENTIAL part of modern transportation system, road network has attracted increasing interests in the practical applications. Road network extraction is not only scientifically challenging but also of major practical importance in military and civilian areas, e.g., map updating [1], navigation, urban evolution monitoring, and disaster relief and response [2]. When handling with these applications, road position needs to be determined first and then those follow-up functions can proceed. Furthermore, road feature, as a low-level feature in image processing and computer vision, is the foundation of many complicated tasks, such as image registration [3] and urban block outlining [4].

With the rapid development of remote sensing techniques, information detection and analysis is becoming an urgent problem. Compared with optical remote sensing, synthetic aperture radar (SAR) has become a suitable tool for road extraction owing to its high spatial resolution and insensitivity to the sun-illumination and atmosphere. Considering the degree of automaticity, road detection methods can be divided into two categories: semiautomatic and automatic extraction. The former usually needs human operators provide road seeds, including a searching direction and an initial point, whereas the latter finds the seeds by the system [5]. Although recognition of all types of road is not realistic, methods designed for specific types of road have achieved some success.

To cope with the automatic road detection task, three-level analysis should be considered. 1) Low-level road feature extraction, which aims at extracting information indicating the likelihood of that pixel being on a road. This level generally includes the following methods: line detectors [6]–[8], step edge detectors [9], classification-based methods [10], and template matching [11]. 2) Medium-level road element extraction. In this level, local properties based on the output of the extracted road features are tested for producing qualified seed points (segments), including thresholding technique [6], local Hough [8], hypotheses generating and testing procedure [12], Bayesian analysis [13], etc. This procedure can be skipped from low-level to high-level processing directly. 3) High-level road network construction, which aims at filling the gaps between road elements, discarding false elements, and connecting portions of road candidates from a global perspective. Common approaches in this level include Markov random fields (MRF) [6], snake model-based method [7], dynamic programming [10], genetic algorithm (GA) [14], integer programming [15], etc. Among these methods, global knowledge has been considered. In most cases, cost functions based on some geometrical, radiometrical, and topological rules are designed to generate an optimal connection. The performance of these methods is mainly depended on the quality and quantity of the extracted road seed elements. If the number of the extracted road seed elements decreases, the computational time will be reduced along with the deterioration of completeness

Manuscript received January 08, 2014; accepted July 12, 2014. Date of publication August 12, 2014; date of current version January 21, 2015.

P. Lu, K. Du, and Y. Deng are with the Department of Space Microwave Remote Sensing, Institute of Electronics, Chinese Academy of Sciences (IECAS), Beijing 100190, China (e-mail: lupp_1989@yeah.net; dukangning11@mails.ucas.ac.cn; ykdeng@mail.ie.ac.cn).

W. Yu is with the Department of Microwave Remote Sensing, Institute of Electronics, Chinese Academy of Sciences (IECAS), Beijing 100190, China (e-mail: ywdsar@yahoo.com.cn).

R. Wang is with the Department of Airborne Microwave Remote Sensing System, Institute of Electronics, Chinese Academy of Sciences (IECAS), Beijing 100190, China (e-mail: yuwang@mail.ie.ac.cn).

T. Balz is with the State Key Laboratory of Information Engineering in Surveying, Mapping, and Remote Sensing, Wuhan University, Wuhan 430079, China (e-mail: balz@whu.edu.cn).

Color versions of one or more of the figures in this paper are available online at http://ieeexplore.ieee.org.

Digital Object Identifier 10.1109/JSTARS.2014.2340394

and location accuracy. However, too much redundancies and false detections will lead to the dramatic increasing of the computational time.

The basic concept of region growing, which is a classical image segmentation method, is grouping pixels or subregions into larger regions based on predefined growth criteria. This method is quite flexible, since one or more criteria can be selected freely according to the characteristics of an image. This concept has been adopted in road extraction task by some researchers, which are usually pixel-based growing method in optical or DSM data [16], [17]. In [14], region growing is used to connect some neighboring road parts in order to speed up the process of GA for road extraction in SAR images. Since SAR images suffer from speckle noises, pixel-based region growing methods not work well in SAR images [18]. In comparison, better performance can be expected letting reliable road seed elements extend in the form of long strips based on rules in geometric and radiometric characteristics. Through this way, the road network extraction method will have better adaptability and can be applied to images with different quality.

In order to automatically, quickly, and adaptively extract road network, a new road network extraction method based on region growing is proposed in this paper. The basic idea is that a road "grows" from the endpoints of automatically selected seeds and "extends" step-by-step in the form of a long strip. In this process, some strategies are incorporated to ensure those road seeds "grow healthy." To enhance the quality of road seeds, an improved ratio line detector W-RLD is put forward and the corresponding outputs, ratio and direction information, are fused to extract road seed regions. To improve the applicability and efficiency of the region growing process, a fast and adaptive growing parameter estimation method is proposed. The remainder of this paper is organized as follows: In Section II, the details of the whole framework are described; in Section III, the analysis of the experimental results is presented; and in Section IV, the conclusion of this paper is made.

II. Methods

To obtain a vector format of the road network from SAR images automatically, four steps are considered: 1) road features extraction procedure to enhance the road characteristics; 2) road seeds generation procedure to yield road elements with a high possibility of belonging to the true road network; 3) road elements linking procedure to give the global connection; and 4) postprocessing procedure to generalize the road network. A flowchart is shown in Fig. 1.

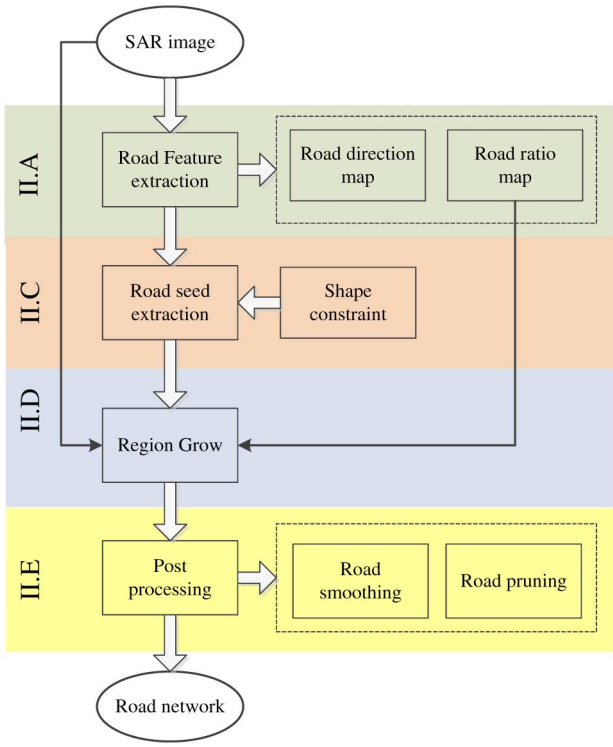

Fig. 1. Block scheme of the proposed procedure.

A. Road Feature Extraction Based on W-RLD

There is a widely used line detector proposed by Tupin *et al.*, which merges the ratio line detector (RLD) and cross-correlation line detector (CCLD) through an associative symmetrical sum [6]. The former denotes the statistical mean as the average radiometry of a considered region, which may be affected by isolated bright points or small regions. The latter considers the variances of the considered regions, which can ease the influence by isolated bright areas. However, both of them are sensitive to the sizes of the central and lateral window and suffer from multiple responses to structures [6]. Since our aim is to deal with the roads extraction in urban areas extraction, the densely distributed buildings and road networks may aggravate the difficulty of the road detection task.

It has been proven that the ratio of exponentially weighted averages (ROEWA) operator, a constant false alarm rate (CFAR) step-edge detector, has better performance than other step-edge operators in images that approximate the multiedge model [19]. Instead of using statistical averages, this operator using a pair of recursive filters computes the exponentially weighted averages on the opposite sides of the central pixel. Then, the normalized ratio of the weighted averages is used for creating the edge strength map. Here, the concept of weighted average is incorporated in road feature extraction procedure to make the aforementioned classical RLD applicable to complex scenes.

In this paper, we used a weighted ratio line detector (W-RLD) based on the concept of weighted averages. Since road can go in any directions, road feature will be computed in different directions. Let $\theta_k = 180\frac{k}{N_0}$, $k = 0, 1, \ldots, N_0 - 1$ be the angles of each direction with the vertical axis [shown in Fig. 2(a)], and N_0 is the number of the total directions and it can be chosen through the tradeoff between the computational accuracy and efficiency. In our experiments, N_0 is set to 18. The W-RLD detail procedures are presented below.

First, we rotate the original SAR image by θ_k in a counterclockwise direction around its center point [shown in Fig. 2(b)]. Then, the convolution between the rotated image I_{θ_k} and an infinite symmetric exponential filter (ISEF) f_y [19]

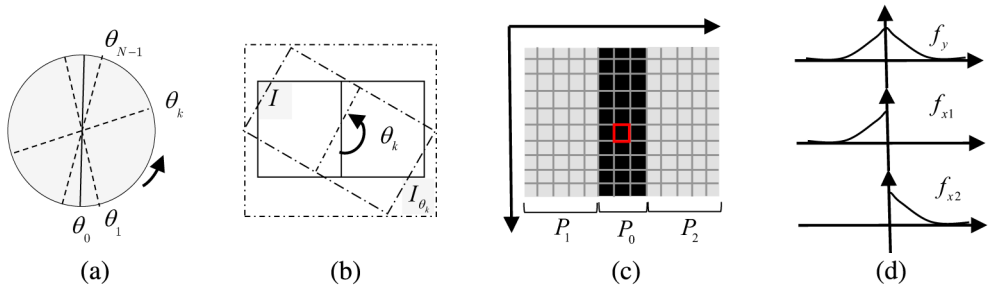

Fig. 2. Schematic representation of the weighted ratio line detector. (a) Division of road direction, (b) the rotation of the original image, (c) definition of the window used by line detector, and (d) the impulse response of weighted functions.

is calculated as the weighted radiometric average of the central window P_0 by

$$I_{p_0}(h,w,\theta_k) = f_y(h) * I_{\theta_k}(h,w) \tag{1}$$

where $*$ represents convolution.

Secondly, I_{p_0} is filtered with a pair of filters f_{x1} and f_{x2}, respectively, i.e.,

$$I_{p_1}(h,w,\theta_k) = f_{x1}(w-t) * I_{p_0}(h,w-t,\theta_k) \tag{2}$$

$$I_{p_2}(h,w,\theta_k) = f_{x2}(w+t) * I_{p_0}(h,w+t,\theta_k) \tag{3}$$

where t equals the half-road width, which can be set according to the resolution of the original image and the real width of roads. This parameter can take different values in order to delineate different road widths. The outputs $I_{p_2}(h,w,\theta_k)$ and $I_{p_2}(h,w,\theta_k)$ are computed as the weighted means of the lateral windows P_1 and P_2. The impulse responses of f_y, f_{x1}, and f_{x2} are displayed in Fig. 2(d).

The calculation process of (1)–(3) can be very efficient through recursive filters, and the detailed information about the structure and parameter setting of recursive filters can be found in [19].

Thirdly, ratio is computed by

$$r_{\theta_k}(h,w) = \max\left(\frac{I_{p_0}(h,w,\theta_k)}{I_{p_1}(h,w,\theta_k)}, \frac{I_{p_0}(h,w,\theta_k)}{I_{p_2}(h,w,\theta_k)}\right). \tag{4}$$

Then, we rotate r_{θ_k} by θ_k in a clockwise direction, the output is denoted as r'_{θ_k}. The pixels with higher values are less likely being on a road.

Finally, the road ratio map R and road direction map φ are derived by the minima of the ratio maps and their corresponding angles, respectively,

$$R(h,w) = \min_{k=0:N_0-1}\left\{r'_{\theta_k}(h,w)\right\} \tag{5}$$

$$\varphi(h,w) = \arg\min_{\theta_k,k=0:N_0-1}\left\{r'_{\theta_k}(h,w)\right\}. \tag{6}$$

B. Road Assumption and Modeling

To obtain a complete road network, the fragments produced by direct thresholded results of the ratio map are unsatisfactory. More subsequent procedures are needed to extract road candidates, such as discarding false-alarm elements and connecting correct parts. However, due to the diversity of road types, a single approach cannot fit for every situation. To continue our subsequent procedures, some necessary assumptions are made as follows [20], [21]: 1) road is visible and distinguishable from the background in the SAR image; 2) the regions belonging to the same road have similar intensity and width; 3) the direction of a road changes slowly, so that we can use piecewise linear function to approximate; and 4) the length and width of any road are limited in SAR images. All of these assumptions are based on the geometrical and radiometric characteristics and need to be combined to get a complete road network. In this paper, a road is considered as the combination of series of end-to-end linear elements and will be described parametrically with the coordinates of endpoints and direction of each linear element, as shown in (7) and Fig. 3

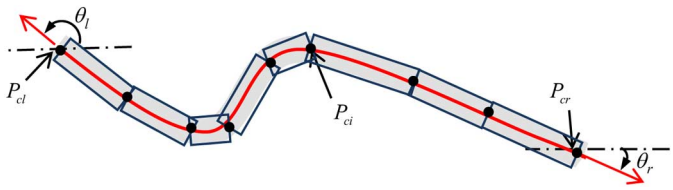

Fig. 3. Road model.

$$L_c = \{P_{cl}, \ldots, P_{ci}, \ldots, P_{cr}, \theta_l, \theta_r\} \tag{7}$$

where P_{cl} and P_{cr} stand for the coordinate of the two endpoints of L_c, P_{ci} represents the ith intermediate points, θ_l and θ_r stand for the corresponding direction of the two endpoints.

C. Road Seed Extraction Based on Feature Fusion

The proposed road network generation method consists of two main parts, road seed extraction and region growing of these extracted seeds. This part gives the details about the first task, the automatic road seed extraction.

1) Extraction of Road Seed Segments: The performance of region growing algorithm is sensitive to the accuracy and distribution of the selected seeds, so an accurate method to extract the road seed is necessary. In Section II-A, two kinds of information have been obtained: one is the ratio map, which indicates the probability of pixels being on a road, and the other is the direction map, which represents the direction trend of a road. To merge these two types of complementary information [22], three criteria are incorporated here: 1) the mean ratio of the region is less than a given ratio threshold; 2) the dynamic range of the direction in this region is smaller than a given direction threshold; and 3) the length of the region is larger than a given minimum road length. If a

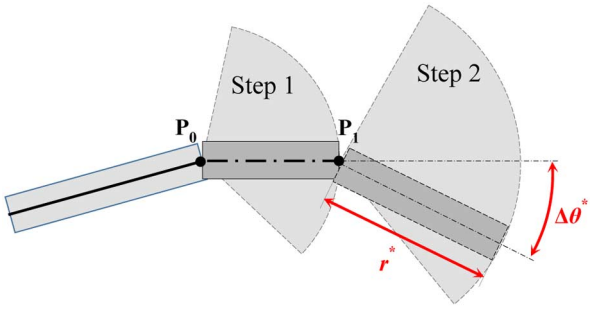

Fig. 4. Road growing procedure.

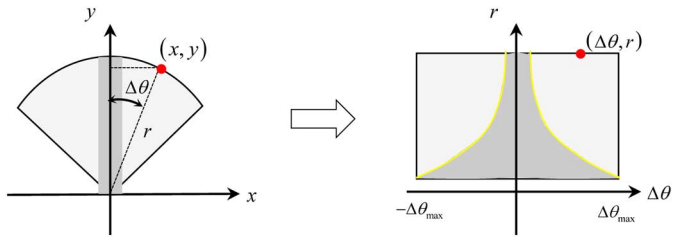

Fig. 5. Transformation of parameter coordinate system and 2-D Cartesian coordinate system.

candidate road seed element satisfies the above three criteria, it is classified as an element of the true road map.

To meet the requirements (1) and (2), a series of masks $\{M_i | i = 0, \ldots, L-1\}$ are obtained by

$$M_i(h, w, \theta_i) = \begin{cases} 1, & R(h,w) < R_{th}, \varphi(h,w) \in [\theta_i - \Delta\theta_M, \theta_i + \Delta\theta_M) \\ 0, & \text{otherwise} \end{cases} \tag{8}$$

where R_{th} is a ratio threshold, $\theta_i = 180\frac{i}{N_1}$, $i = 0, 1, \ldots, N_1 - 1$ and $\Delta\theta_M$ describe the center value and the half width of the direction interval. To simplify the selection of parameters, we make N_1 equal the numbers of angle interval N_0, which has been used in the previous feature extraction part, and make $\Delta\theta_M$ equal zero.

Then those connected components in each mask are extracted as road seed candidates. The shape constraint (3) is checked after completing the vectorization procedure. In our paper, the minimum length is set to be 100 m. In the experimental part, the quality of these road seed elements will be testified.

2) Road Seed Elements Vectorization: A vectorization procedure to implement global construction is needed and several parameters, including the coordinates and directions of its two endpoints, should be estimated as the initial input of the subsequent region growing process.

As mentioned before, a road is modeled as a series of end-to-end linear elements. In the vectorization process, skeletonization is implemented first, then piecewise straight line approximation follows. The first step is a skeleton pruning method based on discrete curve evolution (DCE) proposed by Bai *et al.* [23]. In the second step, Ramer–Douglas–Peucker (RDP) algorithm [24] is adopted to approximate a curve by a series of points using iterative end-point fit. Then, several parameters including the location and direction of its endpoints are estimated.

D. Road Network Extraction Based on Region Growing

The following part depicts the details of region growing-based road network construction method. Fig. 4 shows a typical growing process of a given road seed. A road seed will be extended step-by-step in the form of long strip. The main problem is finding suitable growing parameters, including growing directions and step lengths.

Well-defined region growing criteria are responsible for the final region growing outputs. Generally, we can use four types of information: SAR image intensity, the road ratio map, the road direction map, and the existing road elements, which have been confirmed to be parts of the true road. Since the values of the direction map are vague at the intersection of roads, the growing criteria will mainly depend on the other three types of information. In order to find the optimal growing parameters for a given road seed, the average intensity value of each long strip, defined by every possible $(r, \Delta\theta)$, can be calculated. The parameters where the minimum arrives will be the optimal growing parameters. However, the calculation amount would take too long to be acceptable. In order to solve this problem, a fast-searching method based on ratio map R is proposed here instead.

1) Parameter Space: Instead of searching in the 2-D Cartesian coordinate system, the optimal parameters will be searched in a parameter coordinate system whose axes represent the growing directions $\Delta\theta$ and growing step lengths r. The transformation of these two coordinate systems is shown in Fig. 5. The parameter coordinate system can be inversely transformed into 2-D Cartesian coordinate system by

$$\begin{cases} x = r \sin \Delta\theta \\ y = r \cos \Delta\theta \end{cases} \tag{9}$$

where $r \in (r_{\min}, r_{\max})$ stands for the growing step lengths, and $\Delta\theta \in (-\Delta\theta_{\max}, \Delta\theta_{\max})$ represents the searching directions.

To obtain the optimal growing parameters of any given road seed, the searching area in the Cartesian coordinate system needs to be rotated and translated according to the location and direction of endpoints of the road seed, i.e.,

$$\begin{cases} x' = x_0 + x \cos\theta_r + y \sin\theta_r \\ y' = y_0 - x \sin\theta_r + y \cos\theta_r \end{cases} \tag{10}$$

where $\mathbf{P} = (x_0, y_0)$ and θ_r stand for the coordinates and direction of one of the endpoints of the road seed, respectively. Thus, we can get the ratio information ϕ around $\mathbf{P}$ through interpolation operation in ratio map, i.e.,

$$\phi(\mathbf{P}, \theta_r, \Delta\theta, r) = R(x', y') \tag{11}$$

where $R(x', y')$ represents the value of ratio map at (x', y'). To guarantee the computation efficiency, the sampling intervals of the growing steps and angles are 1 and $\frac{1}{r_{\max}}$, respectively.

2) Weighted Processing: To avoid the excessive offset in direction $\Delta\theta$ and prevent falling into local minima in r, a weighted function will be introduced here. The weights will increase gradually along with increasing angle offset and reduce with the decreasing of growing steps. The specific weighted operation is given by

$$w(z,k) = \frac{2}{1+e^{-k|z|}} \tag{12}$$

$$\phi_w(\mathbf{P},\theta_r,\Delta\theta,r) = R(x',y')w\left(\frac{\Delta\theta}{\Delta\theta_{\max}},k_\theta\right)w\left(\frac{r}{r_{\max}},k_r\right) \tag{13}$$

where k_θ and k_r are set to 0.5 and -0.5, respectively, in this paper. In order to preserve the real structure of the original image, the absolute values of these two factors should be less than 1.

3) Optimal Growing Parameters Estimation: For the purpose of establishing connection between the value of each point in the parameter space and the probability of the existence of road, we need to calculate the average ratio value of each long strip in Cartesian coordinate system. Since the response of a road in the ratio map R has the lowest values along its centerline, a long strip (shown in Fig. 5) in intensity image is simplified as a long line in R. Thus, we calculate the average of the weighted ratio map ϕ_w in parameter coordinate system by

$$\phi'_w(\mathbf{P},\theta_r,\Delta\theta,r) = \frac{1}{r}\sum_{t=1}^{t=r}\phi_w(\mathbf{P},\theta_r,\Delta\theta,t). \tag{14}$$

After transforming the ratio map to the parameter coordinate system, the problem of searching the optimal growing parameters is simplified to find the corresponding parameters $(\Delta\theta^*, r^*)$ where the minimum of ϕ'_w arrives, i.e.,

$$(\Delta\theta^*,r^*) = \underset{r\in[r_{\min},r_{\max}],\Delta\theta\in[-\Delta\theta_{\max},\Delta\theta_{\max}]}{\arg\min}\{\phi'_w(\mathbf{P},\theta_r,\Delta\theta,r)\}. \tag{15}$$

If the minimum is less than the given threshold R_{th}, which has been used in previous road seed extraction part, the new road elements generated by the obtained parameter $(\Delta\theta^*, r^*)$ are added to the road seed, and the parameters of this road seed will be updated.

4) Cocurvilinearity Check: All of the endpoints of these road seeds will grow one time simultaneously. Instead of proceeding the growing procedure for the second time, cocurvilinearity check will be carried on among these newly grown road parts. Those cocurvilinear parts are merged and thus the computation complexity of the whole growing procedure is reduced. The concept of perceptual grouping [14] is included here. In [14], two road seeds will be merged to a new one if their endpoints are close enough to each other and the value of cocurvilinearity measurement (16) is higher than a given threshold TH_c. Besides, if the growing trends of several individual road seeds are consistent, one of them will be allowed to continue growing and the others will be prevented from growing

$$C = \frac{1}{((\tan A)^2+(\tan B)^2)(1+\alpha G)} \tag{16}$$

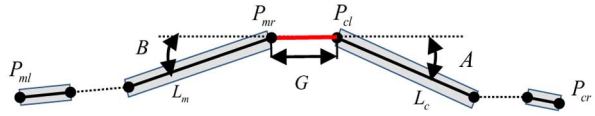

Fig. 6. Perceptual grouping factors: cocurvilinearity.

where α is a controlling parameter, which determine the sensitivity to the length of gap G. A and B (as shown in Fig. 6) are the tangent angles of segments at joined endpoints, as shown in Fig. 6. In this paper, the threshold TH_c is set to 2 and the controlling parameter α is set to 0.05, the smaller the value of α is, the less influence is caused by the gap.

The complete region growing-based road network algorithm is presented in Table I. The required information of this part is given, and the detailed steps are listed one by one.

E. Postprocessing of the Network

After the region growing procedure, short roads have been spread, and those cocurvilinear parts have been merged to form a new elongated road. Although the region growing and cocurvilinearity check can perform well, there are still some defects, including overgrowing, undergrowing, and unevenness of the centerlines for road candidates, which can be overcome mostly through several conventional but effective steps. The first step is a data smooth algorithm, Robust LOcal regrESSion (RLOESS), which is a local regression model using weighted linear least squares and a second degree polynomial model. This algorithm is adopted here to filter and smooth the centerlines of extracted roads. The second step is a road pruning method. Roads will be spread in their corresponding direction starting from one endpoint, and then the nearest crossing point to this endpoint will be picked. If the distance between these two points is less than a given length, the nearest cross-point is classified as a new endpoint of this road. In this way, the end of a road will be spread or cut off to obtain a more regularized road network. The final step is to extract the road junctions, and the crossing point of two different roads will be extracted considering both the length and direction of the two roads.

III. Experimental Results

A. Data Set

To verify the performance of the proposed method, four kinds of SAR images have been tested, including Sendai city (Japan) acquired by TerraSAR-X sensor under strip-map mode with 1.9 and 3.3 m resolution in range and azimuth direction, respectively, a suburban area in Wuhan (China) obtained by HJ-1-C SAR sensor with the spatial resolution of 5 m, parts of the Dujiangyan area acquired by an airborne SAR sensor designed by the Institute of Electronics, Chinese Academy of Sciences (IECAS), with 0.5 m resolution in both range and azimuth direction and one Envisat ASAR image covering Beijing with a spatial resolution of 30 m. Fig. 7 shows the original SAR images and the corresponding true road network extracted manually.

TABLE I
REGION GROWING-BASED ROAD NETWORK EXTRACTION

Requirement	road seeds, ratio map
	region growing parameters, including the maximum length r_{max} and minimum length r_{min}, the range of searching direction $\Delta\theta_{max}$ and a threshold R_{th};
(1).	Cocurvilinearity check and boundary check, count the total number of the active endpoint, denoted as N, if N equals zero, the region growing procedure will stop, otherwise, i will be set to zero and continue;
(2).	$i = i+1$, If $i \le N$ and $N > 0$, continue, else, step to (1);
(3).	Region growing for each active endpoint: the optimal growing parameters will be calculated according to Eq. (13)-(15). Then the minimum of these weights will be compared with the given threshold R_{th}. If the minimum is less than R_{th}, continue, else mark this endpoint as a dead point and step to (2).
(4)	Parameter update of road seed: add the new fragment to this road and replace the endpoint of the old road by the endpoint of the new fragment. Continue at step (2).

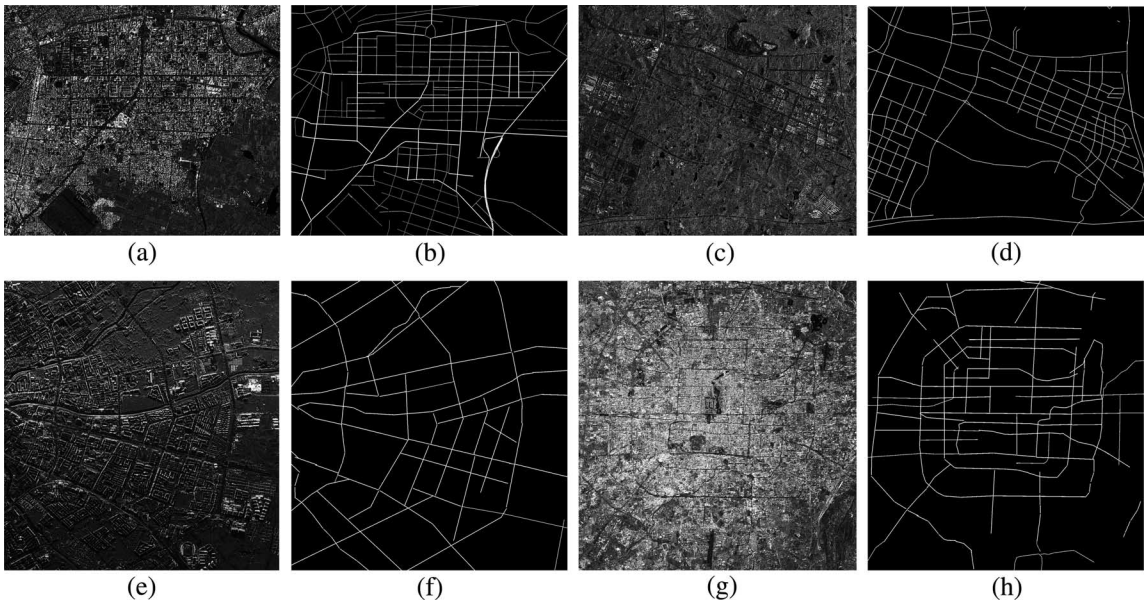

Fig. 7. (a) Sendai area with TerraSAR-X sensor. (b) True road network extraction manually of (a). (c) Wuhan area with HJ 1-C sensor. (d) True road network extraction manually of (c). (e) Dujiangyan area with airborne SAR sensor. (f) True road network extraction manually of (e). (g) Beijing area with Envisat ASAR. (h) True road network extraction manually of (g).

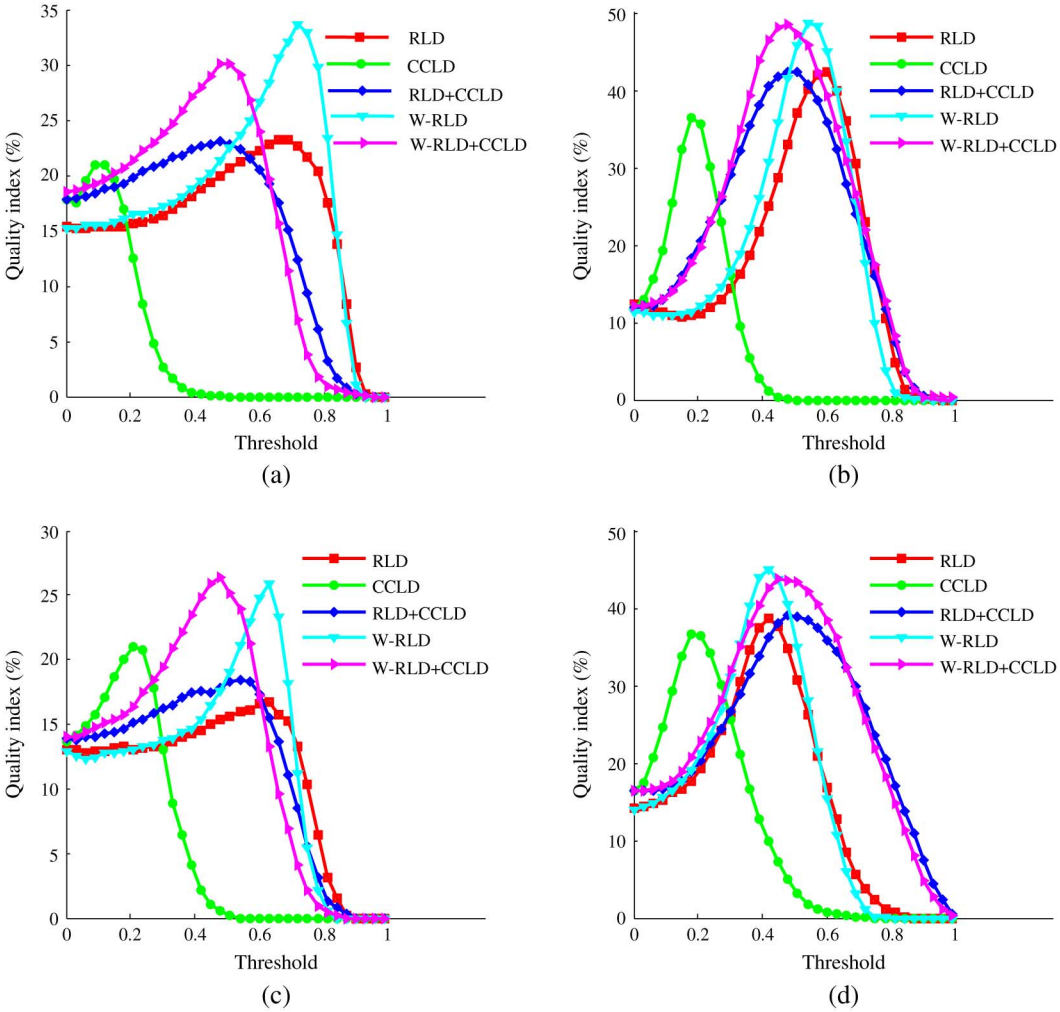

Fig. 8. Performance comparison of different feature extraction methods. (a)–(d) Quality of the thresholded ratio map of Fig. 7(a), (c), (e), and (g).

B. Results and Analysis

The external evaluations of the obtained results are important for an automatic system [25]. Besides visual inspection, several quantitative indexes, including correctness, completeness, and quality [21], will be calculated to confirm the visual analysis. Completeness represents the proportion of the correctly extracted road length to the total length of the ground truth, while correctness evaluates the proportion of the correctly extracted road length to the total length of the extracted road. Finally, quality weights both correctness and completeness in an overall accuracy evaluation. To match the extracted road with the reference, the so-called "buffer method" is adopted, which is a typical matching procedure, and every portion of one network within a given distance from the other network is considered as matched. In our paper, the buffer is set to 5 pixels.

1) Performance of the W-RLD: To testify the performance of the proposed W-RLD, a series of the ratio maps are generated by different road feature extraction methods with similar parameters and then they are converted to binary images under different thresholds. These binary images are evaluated with the corresponding manually extracted road network, and the experimental results are displayed in Fig. 8. Through the comparison of the peaks of different curves, we can see the curves representing the W-RLD have higher quality indexes, compared with RLD, CCLD as well as the fused result of RLD and CCLD. The integrated results of W-RLD and CCLD are shown in magenta curves, and the performance does not improve much compared with W-RLD method alone. So, in the latter experiments, we only adopt W-RLD as the road feature extractor in our paper.

2) Evaluation of Road Seeds: To obtain an acceptable road growing result, the quality of the extracted road seeds should be guaranteed. The road seed generated by our approach considers both shape constrains and intensity contrast with its backgrounds, and the quantitative evaluation results are listed in Table II. The high correctness of the road seeds provides a good foundation for the next growing part.

3) Region Growing Procedure: We take two road seeds as an example to illustrate the specific process of region growing. These two road seeds are from the airborne SAR image, shown in Fig. 7(e). Fig. 9 displays the growing results, and four

TABLE II
QUANTITATIVE EVALUATIONS AND COMPARISON OF THE ROAD SEEDS

	Fig. 7(a)	Fig. 7(c)	Fig. 7(e)	Fig. 7(g)
Completeness	0.35	0.51	0.56	0.44
Correctness	0.91	0.97	0.86	0.94

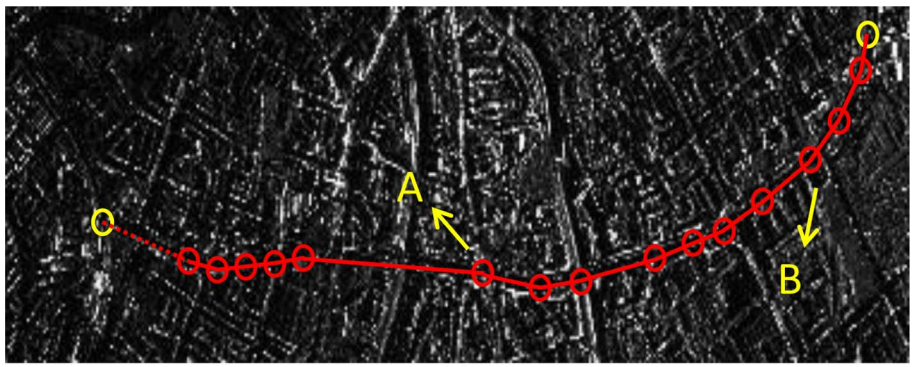

(a)

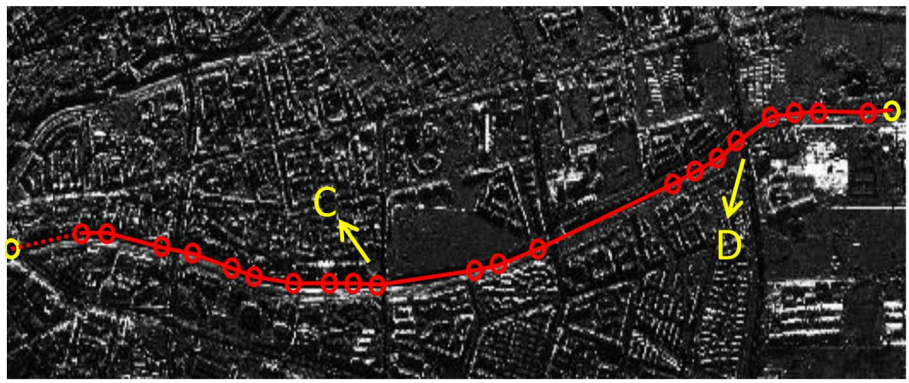

(b)

Fig. 9. Illustration of road growing procedure. The dotted lines indicate the road seeds, the solid lines shows the growing results, and the red circles stand for the intermediate nodes of region growing.

points have been selected to analyze the parameters selection. Points B and C are located in a straight line and their growing steps should be large. Points A and D are located in the bend of a road, and the growing parameter should be carefully selected to avoid overgrowing. The first column of Fig. 10 shows the local ratio map ϕ_w transformed from the Cartesian coordinate system to the parameter coordinate system, and the corresponding cumulative results ϕ'_w are shown in the second column of Fig. 10. The curves in the final column give values along the corresponding optimal growing direction of ϕ_w and ϕ'_w. The growing result shows the adaptability of our proposed fast parameter selection method.

4) Evaluation of Road Network: To evaluate the performance of the final road network visually, images combining the extracted network and the reference are displayed in Fig. 11. Besides, the quantitative measurement of the extracted network is shown in Table III. The experimental result of HJ-1-C SAR image in Wuhan area has the best performance, and the quality index is 83.9%. Since it covers both urban and rural areas, it shows the best performance of the proposed region growing method. Due to the coarse resolution of the Envisat ASAR image covering Beijing area, the quantitative index is 67.2%, which is lower compared with the HJ-1-C result. The urban area in Japan acquired from TerraSAR-X under the Stripmap mode has more complex content compared with the other three images. Both the varying road widths and complex direction trend add difficulty to the road detection task. Besides, some road parts have been even occluded by neighboring topographic surfaces. However, most of the main road has been detected correctly and the final quality index which is 59.0%, which is an acceptable result. To speed up the extraction process, the airborne SAR image covering Dujiangyan area has been down-sampled to $2\,\mathrm{m} \times 2\,\mathrm{m}$ pixel size. Because of the existence of fences and plants on both sides of the road, the quality index amounts to 68.6% even if it has the finest spatial resolution among the four selected SAR sensors. For SAR image with very high resolution, classification-based feature extraction method will work better

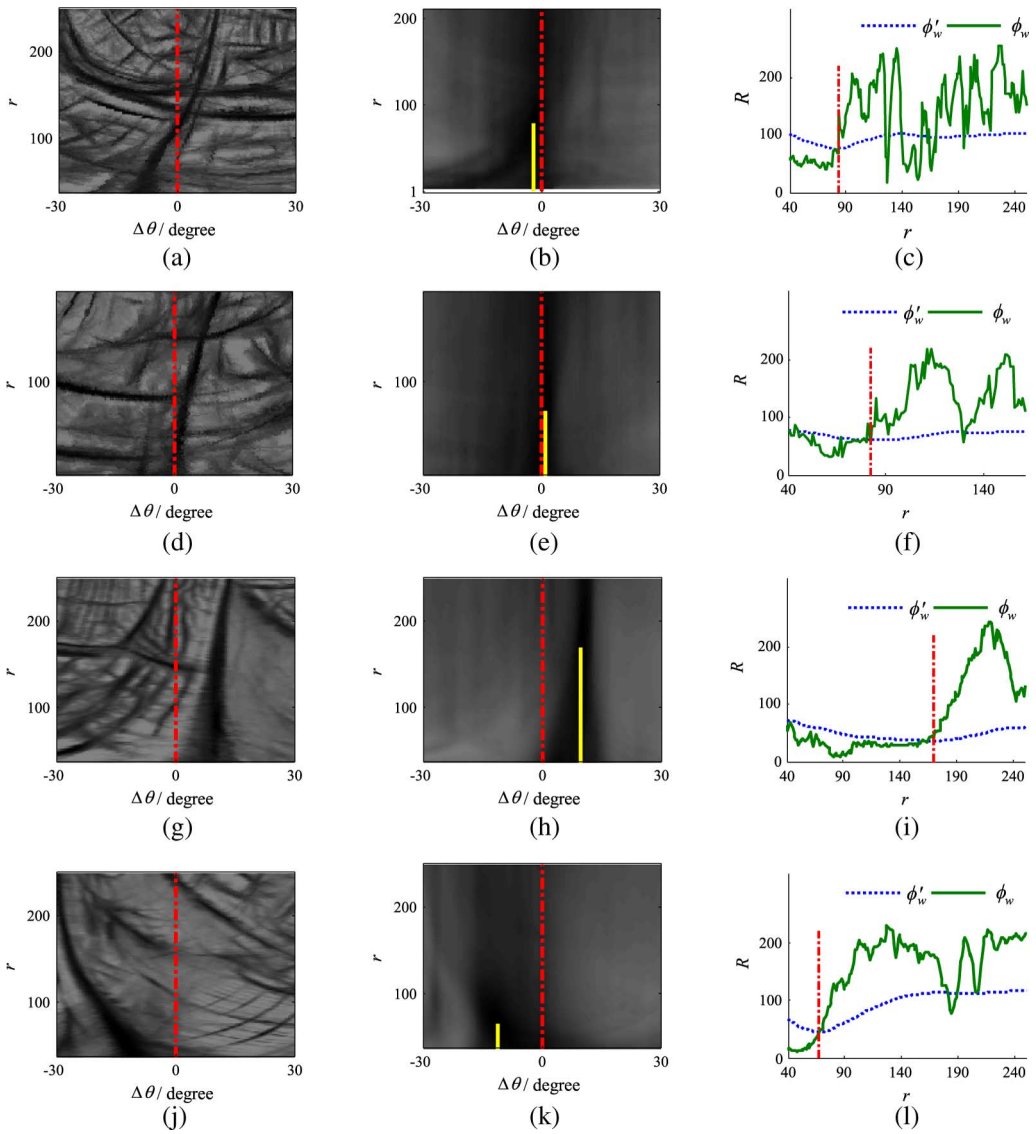

Fig. 10. Optimal growing parameter searching procedure. The first two columns represent the ϕ_w and ϕ'_w of the four points A, B, C, and D shown in Fig. 9, and the curves in the last column correspond to the values ϕ_w and ϕ'_w of in the optimal direction with all steps.

than ratio-based method. Since the data used for the validation of our method have more complex contents than that in other experiments and vary in bands (X band, S band, and C band), it is obvious that our method is robust.

The computational times of the whole processing flow are given in Table IV. These numbers are tested on MATLAB platform, and the corresponding computer is equipped with Intel core i3-3110 quad-core processor, and 4 GB of RAM. From Table IV and Fig. 11, we can see the total time mainly depends on the sizes of the images and the amounts of the contained roads.

For the proposed method, some parameters need to be set by the users depended on the analysis of the data set. Parameters used for the road feature and road seed extraction have been listed and analyzed along with the method description. Table V mainly gives the parameters of the region growing procedure. The maximal searching step $r_{\max}$ influences the running time of the region growing procedure and the positioning accuracy of road parts. A large maximal searching step may increase the searching speed with a reduction of the positioning accuracy and vice versa. Since the bottom of the parameter space will lead to a local minimum, a minimal searching step $r_{\min}$ is needed. The maximal searching angle $\Delta\theta_{\max}$ can be set based on the road curvature and it can take a larger value for image with large-scale scene. The threshold of the ratio map R_{th} is set based on the radiometric contrast between the road part and the background part. Generally, this threshold can be chosen through some automatic operation, automatic thresholding techniques, or just based on experience. Actually, a slight fluctuation will not influence too much on the final output.

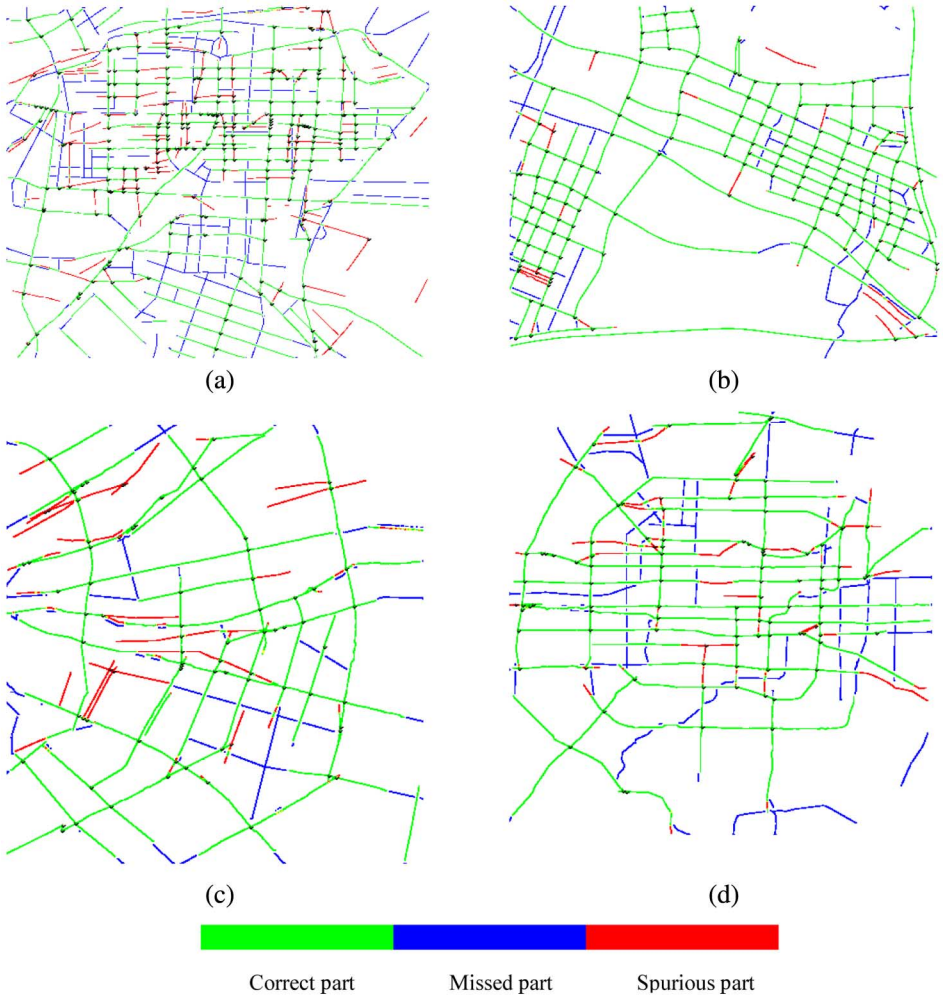

Fig. 11. The final road network extracted by the pro-posed method. (a) Sendai area with TerraSAR-X sensor. (b) Wuhan area with HJ 1-C sensor. (c) Dujiangyan area with aircraft SAR sensor. (d) Beijing area with Envisat ASAR sensor.

TABLE III
QUANTITATIVE EVALUATIONS AND COMPARISON OF THE FINAL RESULTS

	Fig. 11(a) (%)	Fig. 11(b) (%)	Fig. 11(c) (%)	Fig. 11(d) (%)
Completeness	87.4	92.0	86.9	75.2
Correctness	64.4	90.4	76.5	86.3
Quality	59.0	83.9	68.6	67.2

TABLE IV
COMPARISON OF THE COMPUTATION TIME

Type	Size (pixel)	Feature extraction time (s)	Road seed time (s)	Region growing time (s)	Postprocessing time (s)	Total time (s)
Fig. 11(a)	2439*2927	140	112	98	20	370
Fig. 11(b)	1676*2024	92	85	31	13	221
Fig. 11(c)	1462*1388	58	83	10	8	159
Fig. 11(d)	1464*1455	63	46	23	7	139

TABLE V
PARAMETER SETTING

	$\Delta\theta_{\max}$ (^{0})	$r_{\max}$ (pixel)	$r_{\min}$ (pixel)	R_{th}
Fig. 11(a)	30	250	40	0.65
Fig. 11(b)	30	250	40	0.50
Fig. 11(c)	30	250	40	0.60
Fig. 11(d)	40	250	30	0.60

IV. CONCLUSION

We propose a region growing-based automatic network extraction method for SAR images with different resolutions. The proposed improved line feature detector W-RLD has been used for the generation of both road ratio and direction information. Then, the road seed elements have been extracted with high correctness by a feature-fused procedure, providing a guaranteed road seeds for the road network growing. After fully considering the geometric and radiometric characteristics of road in SAR images, a practical method—region growing—has been incorporated in our work. The flexibility of the criteria setting makes it suitable for different types of SAR images with different resolution and changeable contents. The proposed postprocessing method including road centerline smooth and road pruning makes the final road network more regularized. The results of four different images, acquired from different sensors, show the robust and efficiency of our method.

In particular, three improvements are worth stressing.

1) The proposed road feature operator W-RLD replaces statistical averages with weighted averages, which reduces the algorithm's sensitivity to the parameter setting and enhances the ability to delineate the road features.
2) The road seed selection approach proposed in our paper fuses ratio and direction information, and the result shows high values in correctness and provides a guarantee for the next growing part.
3) Region growing-based road network detection method has been presented and a fast growing parameter selection procedure is proposed, which transforms the ratio map from Cartesian coordinate system to parameter coordinate system to adaptively choose the searching step and angle. The adaptability of our method has been validated by four kinds of images acquired from different SAR sensor.

REFERENCES

[1] J. B. Mena, "State of the art on automatic road extraction for GIS update: A novel classification," *Pattern Recognit. Lett.*, vol. 24, no. 16, pp. 3037–3058, 2003.

[2] S. Chen, H. Ma, Y. Fan, F. Xu, and J. Lian, "Road damage assessment from high resolution satellite remote sensing imagery in Wenchuan Earthquake," *J. Remote Sens.*, vol. 6, pp. 6–17, 2008.

[3] F. Dell'Acqua, P. Gamba, and G. Lisini, "Coregistration of multiangle fine spatial resolution SAR images," *IEEE Geosci. Remote Sens. Lett.*, vol. 1, no. 4, pp. 237–241, Oct. 2004.

[4] F. Dell'Acqua, G. Vercesi, and A. Polli, "Urban block outlining in high-resolution SAR images based on detection of linear features," in *Proc. EARSeL*, 2011, pp. 463–471.

[5] S. Kaur, "Automatic road detection of satellite images—A survey," *Int. J. Comput. Appl. Inf. Technol. (IJCAIT)*, vol. 3, no. 2, pp. 32–34, 2013.

[6] F. Tupin, H. Maitre, J. F. Mangin, J. M. Nicolas, and E. Pechersky, "Detection of linear features in SAR images: Application to road network extraction," *IEEE Trans. Geosci. Remote Sens.*, vol. 36, no. 2, pp. 434–453, Mar. 1998.

[7] J. Liu, H. Sui, M. Tao, and X. Mei, "Road extraction from SAR imagery based on an improved particle filtering and snake model," *Int. J. Remote Sens.*, vol. 34, no. 22, pp. 8199–8214, Sep. 2013.

[8] C. He, Z. Liao, F. Yang, X. Deng, and M. Liao, "Road extraction from SAR imagery based on multiscale geometric analysis of detector responses," *IEEE J. Sel. Topics Appl. Earth Observ. Remote Sens.*, vol. 5, no. 5, pp. 1373–1382, Oct. 2012.

[9] G. Cao and Q. Jin, "Automatic detection of main road network in dense urban area using microwave SAR images," *Imag. Sci. J.*, vol. 55, no. 4, pp. 215–222, 2007.

[10] F. Dell'Acqua and P. Gamba, "Detection of urban structures in SAR images by robust fuzzy clustering algorithms: The example of street tracking," *IEEE Trans. Geosci. Remote Sens.*, vol. 39, no. 10, pp. 2287–2297, Oct. 2001.

[11] J. Cheng, Y. Guan, X. Ku, and J. Sun, "Semi-automatic road centerline extraction in high-resolution SAR images based on circular template matching," in *Proc. Int. Conf. Elect. Inf. Control Eng. (ICEICE)*, Wuhan, China, Apr. 2011, pp. 1688–1691.

[12] A. Zlotnick and P. D. Carnine, "Finding road seeds in aerial images," *CVGIP: Image Understanding*, vol. 57, no. 2, pp. 243–260, 1993.

[13] K. Hedman, S. Hinz, and U. Stilla, "Road extraction from SAR multiaspect data supported by a statistical context-based fusion," in *Proc. Joint Urban Remote Sens. Event*, Paris, France, Apr. 2007, pp. 1–6.

[14] B. K. Jeon, J. Jang, and K. Hong, "Road detection in spaceborne SAR images using a genetic algorithm," *IEEE Trans. Geosci. Remote Sens.*, vol. 40, no. 1, pp. 22–29, Jan. 2002.

[15] E. Turetken, F. Benmansour, and B. Andres, "Reconstructing loopy curvilinear structures using integer programming," in *Proc. IEEE Conf. Comput. Vis. Pattern Recognit. (CVPR)*, Portland, OR, USA, Jun. 2013, pp. 1822–1829.

[16] D. Herumurti, K. Uchimura, G. Koutaki, and T. Uemura, "Grid seeded region growing with mixed ART for road extraction on DSM data," in *Proc. IEEE Int. Conf. Signal Process. Commun. Comput. (ICSPCC)*, Hong Kong, China, 2012, pp. 613–617.

[17] D. Herumurti, K. Uchimura, G. Koutaki, and T. Uemura, "Urban road extraction based on Hough transform and region growing," in *Proc. Int. Front. Comput. Vis.*, Incheon, Korean, Jan. 2013, pp. 220–224.

[18] A. E. Carvalho *et al.*, "SAR imagery segmentation by statistical region growing and hierarchical merging," *Digit. Signal Process.*, vol. 20, no. 5, pp. 1365–1378, 2010.

[19] R. Fjortoft, A. Lopes, P. Marthon, and E. Cubero-Castan, "An optimal multiedge detector for SAR image segmentation," *IEEE Trans. Geosci. Remote Sens.*, vol. 36, no. 3, pp. 793–802, May 1998.

[20] C. Han, Z. Zhou, J. Zhu, and C. Ding, "Road extraction from high-resolution SAR image on urban area," in *Proc. IEEE Int. Conf. Geosci. Remote Sens. Symp. (IGARSS'06)*, Denver, CO, USA, Aug. 2006, pp. 1454–1457.

[21] P. Gamba, F. Dell'Acqua, and G. Lisini, "Improving urban road extraction in high-resolution images exploiting directional filtering, perceptual grouping, and simple topological concepts," *IEEE Geosci. Remote Sens. Lett.*, vol. 3, no. 3, pp. 387–391, Jul. 2006.
[22] M. Negri, P. Gamba, G. Lisini, and F. Tupin, "Junction-aware extraction and regularization of urban road networks in high-resolution SAR images," *IEEE Trans. Geosci. Remote Sens.*, vol. 44, no. 10, pp. 2962–2971, Oct. 2006.
[23] X. Bai, J. Latecki, and Y. Liu, "Skeleton pruning by contour partitioning with discrete curve evolution," *IEEE Trans. Pattern Anal. Mach. Intell.*, vol. 29, no. 3, pp. 449–462, Mar. 2007.
[24] D. K. Prasad and M. K. H. Leung, "Polygonal representation of digital curves," in *Digital Image Processing*, S. G. Stanciu Ed. InTech, pp. 71–90, 2012. ISBN: 978-953-307-801-4.
[25] C. Wiedemann, "External evaluation of road networks," *Int. Arch. Photogramm. Remote Sens. Spat. Inf. Sci.*, vol. 34, no. 3, pp. 93–98, Sep. 2003.

Pingping Lu received the B.S. degree in electronic and information engineering from Chinese Agricultural University (CAU), Beijing, China, in 2011. She is currently pursuing the Ph.D. degree at the Department of Space Microwave Remote Sensing System, Institute of Electronics, Chinese Academy of Sciences (IECAS), Beijing, China.

Her research interests include information extraction and change detection of high-resolution synthetic aperture radar (SAR) image.

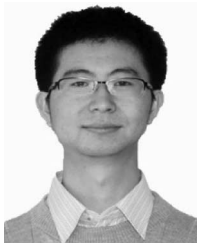

Kangning Du received the B.S. degree in communication engineering from Beijing Information Science and Technology University (BISTU), Beijing, China, in 2011. He is currently pursuing the Ph.D. degree at the Department of Space Microwave Remote Sensing System, Institute of Electronics, Chinese Academy of Sciences (IECAS), Beijing, China.

His research interests include synthetic aperture radar (SAR) image information extraction and analysis.

Weidong Yu (M'00) was born in Henan, China, in 1969. He received the M.Sc. and Ph.D. degrees in electronic engineering from the Nanjing University of Aeronautics and Aerospace, Nanjing, China, in 1994 and 1997, respectively.

Since 1997, he has been with the Institute of Electronics, Chinese Academy of Science (IECAS), Beijing, China, and became a Professor of Communication and Information System in 2000. He has been the Chief Designer of several SAR systems and is currently the Deputy Director of the Department of Space Microwave Remote Sensing System, IECAS. He has published more than 50 papers and is the holder of five patents. His research interests include airborne and spaceborne synthetic aperture radar (SAR) system design and their signal processing.

Robert Wang (M'07–SM'12) received the B.S. degree in control engineering from the University of Henan, Kaifeng, China, in 2002, and the Dr. Eng. degree from the Graduate University of Chinese Academy of Sciences, Beijing, China, in 2007.

In 2007, he joined the Center for Sensorsystems (ZESS), the University of Siegen, Siegen, Germany. He has been involved in the following projects: TerraSAR-X/PAMIR hybrid bistatic SAR experiment, PAMIR/stationary bistatic SAR experiment, PAMIR/stationary bistatic SAR experiment with nonsynchronized oscillators, 3-D/4-D SAR tomography for high-resolution information extraction and monitoring earth's dynamics, millimeter-wave FMCW SAR data processing, and so on. In addition, he has been involved in some SAR projects for Fraunhofer-FHR. Since 2011, he has been a Research Fellow with the Spaceborne Microwave Remote Sensing System Department, Institute of Electronics, Chinese Academy of Sciences (IECAS), where he was currently funded by "100 Talents Programme of the Chinese Academy of Sciences." Since 2012, he is the Coprincipal Investigator (PI) for the Helmholtz-CAS Joint Research Group concerning Space-borne Microwave Remote Sensing for Prevention and Forensic Analysis of Natural Hazards and Extreme Events. His research interests include monostatic and bistatic SAR imaging, high-resolution spaceborne SAR system and imaging model, FMCW SAR system, and millimeter-wave SAR system.

Dr. Wang has contributed to invited sessions at the European Conference on Synthetic Aperture Radar (EUSAR) 2008, 2010, and the European Radar Conference 2009 and IGARSS 2012, 2013, and 2014. He has been chosen as Session Chair at EUSAR2012 and IGARSS2013.

Yunkai Deng (M'xx) received the M.S. degree in electrical engineering from Beijing Institute of technology, Beijing, China, in 1993.

In 1993, he joined the Institute of Electronics, Chinese Academy of Sciences (IECAS), Beijing, China, where he worked on antenna design, microwave circuit design, and spaceborne/airborne SAR technology. He has been the Leader of several spaceborne/airborne SAR programs and developed some key technologies of spaceborne/airborne SAR. Currently, he is a Research Scientist, a Member of the Scientific Board, and the Director of Spaceborne Microwave Remote Sensing System Department, IECAS. His research interests include spaceborne/airborne SAR technology for advanced modes, multifunctional radar imaging, and microwave circuit design.

Timo Balz (M'09) was born in Stuttgart, Germany. He received the Dipl.-Geogr. degree in geography and the Dr.-Ing. degree in aerospace engineering and geodesy from the Universitaet Stuttgart, Stuttgart, in 2001 and 2007, respectively.

From Fall 2001 to the end of 2007, he was a Research Assistant with the Institute for Photogrammetry, Universitaet Stuttgart. From 2004 to 2005, he was a Visiting Scholar with Wuhan University, Wuhan, China. From 2008 to 2010, he has been a Postdoctoral Research Fellow with the State Key Laboratory of Information Engineering in Surveying, Mapping, and Remote Sensing (LIESMARS), Wuhan University. Since 2010, he is an Associate Professor for Radar Remote Sensing with the LIESMARS. His research interests include SAR simulation, surface motion estimation with SAR, computer visualization, SAR image interpretation, and radargrammetry.

Dr. Balz serves as an Associate Editor for the IEEE Geoscience and Remote Sensing Letters, and he is also a member of the Editorial Advisory Board of the ISPRS Journal of Photogrammetry and Remote Sensing.